Aus der Klinik für Psychiatrie und Psychotherapie
(Prof. Dr. J. Wiltfang)
der Medizinischen Fakultät der Universität Göttingen

C-terminally truncated Amyloid-β peptides in Alzheimer's dementia: Deposition of Aβ37, Aβ38, and Aβ39 in the brains of patients with sporadic and familial Alzheimer's dementia and in transgenic mouse models

INAUGURAL-DISSERTATION

zur Erlangung des Doktorgrades
der Medizinischen Fakultät der
Georg-August-Universität zu Göttingen

vorgelegt von

Jochim Reinert

aus

Reinbek

Göttingen 2017

Dekan:	Prof. Dr. rer. nat. H.K. Kroemer
Referent	Prof Dr. O. Wirths
Ko-Referentin:	Prof. Dr. C. Stadelmann-Nessler

Datum der mündlichen Prüfung: 25.01.2018

Hiermit erkläre ich, die Dissertation mit dem Titel "C-terminally truncated Amyloid-β peptides in Alzheimer's dementia: Deposition of Aβ37, Aβ38, and Aβ39 in the brains of patients with sporadic and familial Alzheimer's dementia and in transgenic mouse models" eigenständig angefertigt und keine anderen als die von mir angegebenen Quellen und Hilfsmittel verwendet zu haben.

Göttingen, den …… ……

(Unterschrift)

Table of contents

List of abbreviations

AD	Alzheimer's Disease
APP	Amyloid-β Precursor Protein
Aβ	Amyloid-β
β-CTF	β C-terminal Fragment of APP
CAA	Cerebral Amyloid Angiopathy
DAB	3'3-Diaminobenzidine
DAPI	4'6-Diamidine-2'-Phenylindoldihydrochloride
DS	Down Syndrome
ELISA	Enzyme-linked Immunosorbent Assay
FAD	Familial Alzheimer's Disease
FCS	Fetal Calf Serum
GSM	γ-Secretase Modulator
IF	Immunofluorescence
IHC	Immunohistochemistry
IP	Immunoprecipitation
mAb	Monoclonal Antibody
NDC	Non-Demented Control
NP	Neuritic Plaque
pAb	Polyclonal Antibody
PBS	Phosphate-Buffered Saline
PSEN1	Presenilin1
PSEN2	Presenilin2
PVDF	Polyvinylidenfluorid
SAD	Sporadic Alzheimer's Disease
SDS	Sodium Dodecyl Sulfate
TBS	Tris-buffered Saline
Tris	Tris(hydroxymethyl)aminomethane; 2-Amino-2-(hydroxymethyl)propane-1'3-diol
v/v	Volume-to-volume
w/v	Weight-to-volume
WB	Western Blot
wt	Wildtype

1 Introduction

Alzheimer's disease (AD) is a devastating neurodegenerative disorder of the elderly characterized by progressive cognitive impairment. The disease represents the most common cause of dementia, and the rising prevalence of the disease in aging populations poses significant challenges to societies around the globe. The situation is further complicated by the fact that clinicians still lack effective treatment options that could interfere with disease progression (Blennow et al. 2006). The incidence of the disease has been described as strongly age-dependent: while almost negligible until the age of 60 years, and still below 1% in people aged 60-64 years, the incidence of AD has been reported to show an almost exponential increase with every 5 years after the age of 65 years (Ferri et al. 2005). The world-wide prevalence was estimated at 46.8 million in 2015 and is expected to increase substantially in the future (Prince 2015). While rare single-gene mutations could be identified in cases of familial AD (FAD) that exhibit an autosomal-dominant inheritance and an earlier onset in life, the majority of cases, classified as sporadic AD (SAD), is believed to occur spontaneously. However, several genetic and acquired risk factors for SAD have been described. Notably positive family history of SAD has been found to significantly increase the risk of developing the disease (van Duijn et al. 1991). The Apolipoprotein E ε4 allele has been described as the most important independent genetic risk factor for SAD, which has been validated by studies on both the Framingham and the Rotterdam study cohorts (Corder et al. 1993; Myers et al. 1996; Slooter et al. 2004). Acquired risk factors that have been associated with SAD include vascular disease, hypertension, and hyperlipidemia as well as obesity and physical inactivity. Managing these modifiable risk factors is believed to bear great potential for the primary prevention of SAD (Norton et al. 2014).

Pathological examination of a patient with AD reveals severe brain atrophy that is accompanied histologically by two characteristic hallmarks of the disease: extracellular neuritic plaques (NPs) composed of Amyloid-β (Aβ) and intracellular neurofibrillary tangles that are composed of hyperphosphorylated tau protein. NPs are found in the limbic as well as in the association cortices and axonal and dendritic injury of neurons is typically seen in proximity (Selkoe 2001). In the majority of AD cases concomitant cerebral amyloid angiopathy (CAA), i.e. deposition of Aβ to the vasculature and disruption of the vascular architecture, is observed (Biffi and Greenberg 2011).

In principle, a definite diagnosis of the disease requires post-mortem histopathologic examination, which includes classification of neuropathology according to the Braak stage (Braak and Braak 1991). During lifetime though, careful clinical assessment of every patient with cognitive impairment allows determination of the most likely cause of the deficit in each individual case. Manifest AD typically shows a pattern of memory impairment that is distinctive from other forms of amnesic disorders and can be recognized by experienced

clinicians. In addition, neuropsychological testing, imaging of the CNS, and laboratory tests are applied to rule out other treatable causes of the deficit such as depression, hypothyroidism, or structural diseases of the brain (McKhann et al. 2011; Markowitsch and Staniloiu 2012). Evaluation of cerebrospinal fluid for biomarkers of neurodegeneration, typically Aβ42, total tau, and phospho-tau, may be carried out to increase diagnostic certainty in some cases, but is not routinely applied in the diagnostic procedure. The same holds true for the use of currently available methods of nuclear medicine, i.e. FDG-PET and HMPAO-SPECT (Leitlinie Demenzen 2015). As sensitivity and specificity of the described diagnostic procedure is limited, especially in cases of AD with only mild cognitive impairment, possible biomarkers for a better diagnosis of incipient AD are being investigated. In the future more elaborate combinations of cerebrospinal-fluid (CSF) markers, as well as specific Aβ-specific imaging, may allow the identification of patients with incipient AD and even individuals at risk of developing the disease (Blennow et al. 2015).

Highlighting the need for accurate diagnostic tools for the diagnosis of incipient AD, neuropathological changes have been found to begin long before obvious cognitive impairment (Villemagne et al. 2013). It is therefore believed that disease-modifying treatments would need to be started early in disease course, as neuropathological changes are assumed to be irreversible (Blennow et al. 2006). While disease-modifying treatments are under development, currently available and recommended drugs can only ameliorate symptoms of the disease. Drugs that are recommended for the use in AD include the Acetylcholine-Esterase-inhibitors Donezepil, Galantamin, and Rivastigmin and the NMDA antagonist Memantine. Considerations before initiation of a therapy include severity of the symptoms and possible side-effects of the respective drugs (Leitlinie Demenzen 2015).

After Aβ peptides were isolated from the vasculature and NPs of AD brains and tangles were found to consist of hyperphosphorylated tau, questions arose about the role of Aβ and tau in pathogenesis of AD (Glenner and Wong 1984; Masters et al. 1985; Gorevic et al. 1986). The amyloid hypothesis was introduced in the early 1990s and proposed that the pivotal abnormality in AD-cases is an altered production of Aβ peptides that induces a cascade of pathologic events in which the accumulation of Aβ peptides precedes hyperphosphorylation of tau and formation of neurofibrillary tangles (Hardy and Allsop 1991; Hardy und Higgins 1992).

At first the concept of the amyloid hypothesis was essentially based on the recognition that the gene encoding the Amyloid-β precursor protein (APP) had been found to be located on chromosome 21 (Kang et al. 1987; Tanzi et al. 1987) and that individuals with trisomy 21 (Down Syndrome; DS) were known to present AD-typical neuropathology at a young age (Olson and Shaw 1969). Further evidence for the hypothesis comes from studies on FAD cases, that were invariably found to be caused by single-gene mutations in genes implicated in the generation of Aβ peptides: the APP gene and the presenilin genes Presenilin 1 (PSEN1) and Presenilin 2 (PSEN2) (Tanzi 2012). A continuing accrual of data suggests that

even subtle changes in Aβ production, especially an increase in the Aβ42:Aβ40 production rate, can facilitate pathogenesis of AD presumably through the formation of toxic oligomers (Haass and Selkoe 2007; Kuperstein et al. 2010).

Although there is still lack of clarity in details, at present it is believed that an imbalance in production and clearance of Aβ peptides is essential for pathogenesis of AD. As reviewed by Hardy and Selkoe in recent years it is now justified to claim that the hypothesis is not only widely accepted, but that concerns with the concept, e.g. the observation that the number of amyloid plaques does not correlate well with cognitive decline, have been met with conclusive explanations and experiments. Furthermore the hypothesis has in fact laid the groundwork for promising therapeutic approaches (Hardy and Selkoe 2002; Selkoe and Hardy 2016).

Aβ proteins are generated by processing of APP. In a first step the single-transmembrane protein APP is cleaved by the β-secretase enzyme. While the N-terminal ectodomain of APP is set free, the C-terminal fragment (β-CTF) remains membranebound. β-CTF undergoes further intramembranous proteolysis facilitated by γ-secretase, which releases a 37-43 amino acid Aβ protein (Haass et al. 2012). Notably the presenilin genes were found to encode for the active site of the γ-secretase (Strooper et al. 1998). This multiprotein complex has been described to determine the C-terminus of Aβ (Beher et al. 2002). The intramembranous proteolysis of β-CTF by γ-secretase is initiated by ε-cleavage, which occurs either at T48 or L49 of β-CTF (Funamoto et al. 2004). Further action of the γ-secretase ensues, with subsequent cleavage at every three to four amino acid residues. It has been speculated that two major product lines of Aβ emerge, in which the initial ε-cleavage would determine the outcome:

$$Aβ49 > Aβ46 > Aβ43 > Aβ40 \text{ and } Aβ48 > Aβ45 > Aβ42 > Aβ38$$

This hypothesis has been established based on the detection of the corresponding tri- and tetrapeptides in vitro (Qi-Takahara et al. 2005; Takami et al. 2009). However, a recent study by Matsumura et al. found the two major product lines to be extensively interlinked by occasional γ-secretase cleavage at every fourth, fifth or sixth residue (Matsumura et al. 2014). This is in line with earlier studies on the generation of the C-terminally truncated Aβ peptide Aβ38, which found the peptide's generation by γ-secretase to be independent from Aβ42 generation (Czirr et al. 2008; Page et al. 2008). In addition, Aβ38 levels in CSF were found to correlate well with levels of Aβ40, while no correlation with Aβ42 levels could be established (Schoonenboom et al. 2005; Gabelle et al. 2010). Furthermore, the generation of the C-terminally truncated Aβ peptides Aβ37 and Aβ39 was demonstrated recently. Aβ39 was found to result mainly from cleavage of Aβ42 as indicated by the detection of the GVV tripeptide. In contrast, Aβ37 was described to either result from cleavage of Aβ42, by release of the GVVIA pentapeptide or from cleavage of Aβ40 by release of the VIA tripeptide (Matsumura et al. 2014).

Interfering with the process of Aβ production by γ-secretase modulation has been suggested as a therapeutic strategy to reduce Aβ accumulation. Putative γ-secretase modulators (GSMs) should influence Aβ production in a way that lowers the production of toxic Aβ species like Aβ42. Importantly, other functions of the γ-secretase should not be compromised by a putative GSM (Czirr and Weggen 2006). The non-steroidal anti-inflammatory GSMs have been demonstrated to selectively decrease production of Aβ42. An effect that is achieved partially by increasing the levels of the C-terminally truncated Aβ species (Weggen et al. 2001; Beher et al. 2002).

A recent study on a C-terminal fragment of Aβ, the hexapeptide Aβ32-37, underscores the importance of Aβ C-terminal truncations, as the fragment was found to be a potent peptide inhibitor of Aβ aggregation. In addition, Aβ toxicity in cell culture was mitigated by the hexapeptide (Bansal et al. 2016).

Passive immunotherapy against Aβ is a promising therapeutic approach for AD and several antibodies targeting Abeta are currently being tested in clinical trials. It is worth noting that the antibodies that entered clinical trials target different epitopes of Aβ and show different binding properties, e.g. to monomeric or oligomeric forms of Aβ and to plaques (Selkoe and Hardy 2016).

Depending on their C-terminus, Aβ peptides exhibit different propensities with longer Aβ species, being particularly prone to accumulation (Jarrett et al. 1993). Ever since the amyloid hypothesis has been put forward, research has focused on Aβ peptides, and studies on the deposition of the presumably most toxic variant Aβ42 and the most produced variant Aβ40 are numerous. Aβ42 has been proposed to be the earliest peptide deposited within NPs and to represent the predominant species in parenchymal depositions of Aβ (Golde et al. 2000). In contrast Aβ40 has been found to be the most abundant species within the vasculature in cases of AD with concomitant CAA (Gravina et al. 1995).

C-terminally truncated Aβ peptides however, have received little attention. Except for a recent study that focused on the deposition of Aβ38 in SAD and FAD cases (Moro et al. 2012), depositions of C-terminally truncated Aβ peptides in AD have not been systematically studied. C-terminally truncated Aβ peptides have been consistently detected within the CSF (Wiltfang et al. 2002; Portelius et al. 2010a). Moreover they were found to be present in human plasma, although at low levels (Maler et al. 2007). It has been suggested that measurement of C-terminally truncated Aβ peptides would increase diagnostic accuracy of CSF sampling for the diagnosis of AD (Struyfs et al. 2015).

The present study aims to investigate the deposition of C-terminally truncated Aβ peptides in AD. It extends earlier findings on Aβ38, which described the peptide to be mainly deposited to the vasculature (Tomidokoro et al. 2010; Moro et al. 2012), and for the first time it describes the predominant location and the severity of depositions of two further C-terminally truncated Aβ peptides - Aβ37 and Aβ39 - in SAD in comparison with non-demented control (NDC) cases. In addition, several cases of FAD, with underlying mutations

in the APP gene or the PSEN1 gene are analyzed. This includes analysis of the just recently described APP mutation I716F, which has not been investigated for deposition of Aβ peptides with different C-termini before (Guardia-Laguarta et al. 2010). The study further investigates a set of commonly used transgenic mouse models of AD for deposition of C-terminally truncated Aβ peptides.

This text summarizes and discusses the results of two publications. While publication I focusses on the depositions of Aβ38 in AD partly confirming and partly disputing earlier findings on the peptide, publication II for the first time analyzes the deposition of Aβ37 and Aβ39 in AD.

2 Patients, Materials and Methods

2.1 Patients

Brain tissue from patients with AD, patients with DS, and NDC cases was used in this study. Written informed consent about the use of their brain tissue for the purpose of research was obtained from each individual or their relatives. Brain tissue was provided by the following institutions: The Netherlands Brain Bank, Hôpital de la Salpêtrière Paris, University Hospital Helsinki, Uppsala Universitet, and Medizinische Universität Wien.

In total, brain tissue from 13 cases of sporadic AD, 9 cases of NDC, 2 cases of AD with additionally diagnosed CAA (AD+CAA), and 3 cases of DS was investigated. In addition, brain tissue from several cases of FAD with underlying mutations in either the APP gene (figure 1) or the PSEN-1 gene was analyzed. The study included analysis of cases of the 'Swedish' APP mutation KM670/671NL (Mullan et al. 1992), the 'Arctic' APP mutation E693G (Nilsberth et al. 2001), the APP mutation I716F (Sieczkowski et al. 2014), as well as the PSEN1 mutations P246L (Campion et al. 1995), L418F (Wirths et al. 2010), and cases of the PSEN1 mutation ΔExon 9 (Perez-tur et al. 1995).

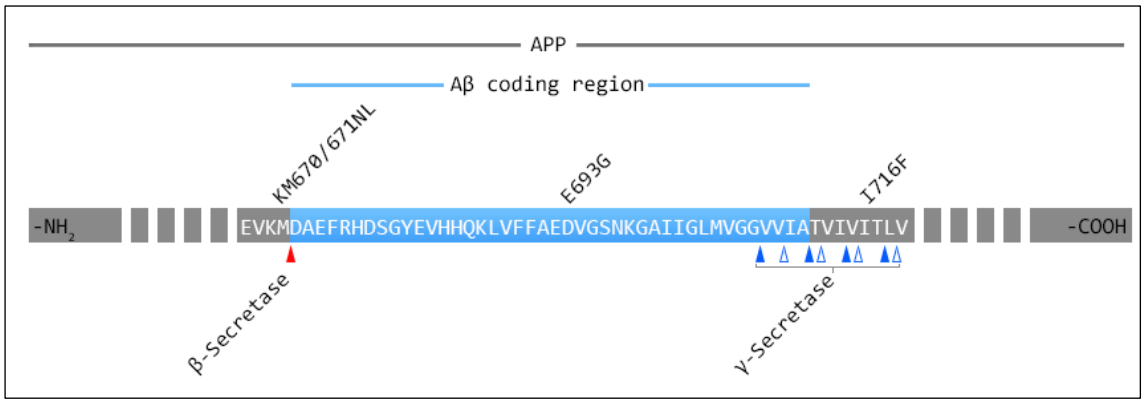

Figure 1: Diagram showing the primary protein sequence of the Aβ coding region within the longer APP and position of the three APP mutations that were analyzed for depositions of C-terminally truncated Aβ peptides in this study. Action of β-Secretase is indicated by a red arrow. Blue arrows indicate the subsequent cleavage by γ-Secretase that was proposed by Qi-Takahara et al. as the underlying mechanism of the generation of Aβ peptides with varying C-termini (Qi-Takahara et al. 2005). Outlined arrows indicate the Aβ49 > Aβ46 > Aβ43 > Aβ40 product line, filled arrows indicate the Aβ48 > Aβ45 > Aβ42 > Aβ38 product line. Figure was made using Adobe Photoshop (Adobe Systems, San José, CA, USA).

Diagnosis was made according to established histopathological criteria. Classification according to Braak-stages, which is based on the severity of taupathology (Braak and Braak 1991), was obtained for the analyzed SAD, AD+CAA, DS and NDC cases.

2.2 Mouse Models

For this study brain tissue from a set of established transgenic mouse models of AD was analyzed. These commonly used mouse models of the disease are known to show an AD-like histopathology with varying degrees of NPs, taupathology and neuron loss. The analyzed models comprised PDAPP (Games et al. 1995), APP23 (Sturchler-Pierrat et al. 1997), 3xTg (Oddo et al. 2003), APP/PSEN1 Ex9 (Garcia-Alloza et al. 2006), 5xFAD (Oakley et al. 2006), and APP/PSEN-KI (Casas et al. 2004).

2.3 Antibodies

The polyclonal affinity purified rabbit anti-Aβ38 antibody #218403 has been generated by Synaptic Systems (Göttingen) using a synthetic peptide LMVGG corresponding to the C-terminus of Aβ38. Antibody specificity was demonstrated by an Enzyme-linked immunosorbent assay (ELISA) and a Dot-blot analysis, which were carried out by Henrik Martens of Synaptic Systems (refer to figure 1C of publication I).

Table 1: Targets, names, suppliers, and types of antibodies used in different experiments. mAb = monoclonal antibody, pAb = polyclonal antibody, IP = Immunoprecipitation, IHC = Immunohistochemistry, IF = Immunofluorescence, WB = Western Blot; Epitope that was used for generation of the antibody in brackets (as stated by the respective supplier), 1=Name of cell line, 2=Catalog number of supplier Synaptic Systems.

Target (Epitope)	Name	Supplier	Type	Use	Dilution in IHC
Aβ (1-16)	6E10[1]	Covance	Mouse mAb	IP	n/a
Aβ (17-2)	4G8[1]	Covance	Mouse mAb	IHC	1:1000
Aβ (N-Terminus)	1E8[1]	Milipore	Mouse mAb	WB	n/a
Aβ 37	D2A6H[1]	Cell Signaling	Rabbit mAb	IHC, IF, WB	1:800
Aβ 38	#218403[2]	Synaptic Systems	Rabbit pAb	IHC, IF	1:250
Aβ 38	326 F1[1]	Synaptic Systems	Mouse mAb	IHC, IF	1:250
Aβ 38	BA1-13[1]	Covance	Rabbit mAb	IHC	1:200
Aβ 39	D5Y9L[1]	Cell Signaling	Rabbit mAb	IHC, IF, WB	1:400
Aβ 40	G210[1]	Milipore	Mouse mAb	IHC, IF, WB	1:1000
Aβ 42	#218703[2]	Synaptic Systems	Rabbit pAb	IHC	1:200

To further confirm specificity of the antibody in an immunohistochemical (IHC) staining, an immunoadsorption protocol was carried out as previously described (Saul et al. 2013). In short, the anti-Aβ38 pAb #218403 was incubated with 1g Aβ4-38 overnight at 4°C under agitation. The supernatant that resulted from 5 min centrifugation at 14,000x g was used for

immunohistochemical stainings in a 6-month-old APP/PSEN1-KI mouse. At the same time an adjacent slice was stained using the antibody without prior immunoadsorption.

2.4 Immunohistochemistry

Paraffin-embedded brain tissue was sectioned into 4µm sagittal sections using a microtome. Sections were mounted onto slides, dried overnight at 37 °C and used for 3'3-diaminobenzidine (DAB) immunohistochemistry (IHC). Sections were deparaffinized in a xylene bath and rehydrated using an ascending series of ethanol baths (70 %, 95 %, and 100 %). To block activity of endogenous peroxidases, sections were incubated for 30 minutes in 0.3 % H_2O_2 in 0.01 M PBS. Antigen retrieval was achieved by two steps: At first sections were boiled in 0.01 M citrate puffer for 10 minutes using a microwave. In a second step, incubation in 88% formic acid was performed following permeabilization with 0.1 % Triton X-100 in 0.01 M PBS. Prior to incubation with primary antibodies, blockage of unspecific binding sites was ensured. Sections were circled with a lipid pen and a blockage solution consisting of 10 % fetal calf serum (FCS) and 4 % skim milk powder in 0.01 M PBS was applied. After incubation of the blockage solution for 1 hour at ambient temperature, the primary antibody diluted in 0.01 M PBS and 10 % FCS was applied to the sections and incubated overnight at ambient temperature. The respective dilution of primary antibodies used in IHC is specified in Table 1. After thorough washing steps, incubation with biotinylated secondary antibodies (DAKO, Glostrup 1:200) in 0.01 M PBS and 10 % FCS was performed at 37 °C for 1 hour, followed by washing steps and application of the ABC method with a Vectastain kit (Vector Laboratories, Burlingame, USA). The ABC solution was produced by adding both components of the kit to 0.01 M PBS containing 10 % FCS. Incubation was carried out at 37 °C for 1.5 hours. After washing steps, staining was revealed by short incubation with a solution containing the chromogen DAB (0.5 mg/ml DAB in 50 mM Tris/HCl with 0.15 ‰ H_2O_2). Hematoxylin was used for counterstaining. Before application of mounting medium and cover slips, the slides were dehydrated using a descending series of ethanol baths (100 %, 95 %, 70 %) and xylene baths.

With a camera-equipped microscope bright field images of the stained sections were acquired. Figures were generated using Adobe Photoshop (Adobe Systems, San José, CA, USA). Semiquantitative analysis of immunoreactivity in each section was performed for NPs and CAA. Aβ staining intensity was rated as follows: - absent staining; (+) scarce staining, + weak staining, ++ moderate staining, +++ abundant staining.

2.5 Immunofluorescence

Immunofluorescence (IF) staining was carried out to evaluate the staining patterns of two different primary antibodies in the same section. Fluorescent secondary antibodies used include DyLight488, Dylight594 (Thermofisher Scientific), and Alexa594 (Invitrogen). 4'6-

diamidine-2'phenylindole dihydrochloride (DAPI, Sigma-Aldrich), which emits at 461nm and shows high binding-affinity to DNA, was used for counterstaining.

2.6 Urea-based SDS-Page and Western Blot

The one-dimensional Urea-based SDS Page and Western Blot was employed to evaluate Aβ species in the 5xFAD transgenic mouse model of AD. The method allows separation of Aβ peptide variants that differ in length by just one amino-acid and was applied as previously described (Wiltfang et al. 1997).

To generate protein extracts, brain tissue from 12-month-old wildtype and 5xFAD mice was homogenized in Tris-buffered Saline (TBS. 120 mM NaCl, 50 mM Tris, pH 7.5) in a weight-to-volume (w/v) ratio of 1:10 with a glass Teflon® homogenizer followed by centrifugation for 20 min at 17,000 x g. The supernatant was separated and termed TBS fraction. After suspending the resulting pellet in TBS and a second centrifugation the final pellet was sonified and dissolved in 2 % sodium dodecyl sulfate (SDS). The lysates were evaluated for protein concentrations with the Roti-Quant® protein assay (Carl Roth), a photometric assay for protein quantitation according to Bradford. Immunoprecipitation (IP) of Aβ peptides from the brain lysates was carried out as previously described (Haussmann et al. 2013; Savastano et al. 2015) using magnetic sheep anti-mouse IgG Dynabeads M-280, that were precoated overnight with the Anti-Aβ mAb 1E8 (Covance) at 4 °C.

Samples of a protein concentration of 2 mg/ml were then prepared in electrophoresis buffer (0.36 M Bistris, 0.16 M bicine, 15 % (w/v) sucrose, 1 % (w/v) SDS, 0,0075 % bromophenol blue) and one-dimensional urea-based SDS-PAGE was applied as previously described (Savastano et al. 2015). 10 µl (equivalent to 20 µg of total protein) of each sample were separated on a urea Bicine/Bis-Tris/Tris-sulfate SDS-polyacrylamide gel (8 M Urea, 10 % T, 5 % C, 0.25 % SDS, 0.4 M H_2SO_4). A standard of synthetic Aβ peptides (Aβ1-37, Aβ1-38, Aβ1-39, Aβ1-40, Aβ1-42) was applied, which served as a reference for the electrophoretic mobility of the different Aβ variants. Western blot onto a PVDF membrane was performed thereafter for 45 min at 1 mA/cm^2 using a discontinuous buffer system. The blot was assembled from the anode to the cathode as follows: 1 filter paper (extra thick blot filter paper, Biorad) that was soaked for 15 min in 0.21 M Tris / 30 % methanol, 1 filter paper that was soaked for 15 min in 25 mM Tris / 30 % methanol, a PVDF membrane that was equilibrated in 25 mM Tris / 30 % methanol, the polyacrylamide gel which was briefly pre-incubated in 25 mM Tris-borate (pH 9.0, 0.025 % SDS), and two filter papers that were soaked in 25 mM Tris-borate (pH 9.0, 0.025 % SDS). After the blotting was completed the PVDF membrane was boiled for 3 min in PBS using a microwave oven to facilitate the immunodetection (Ida et al. 1996). Prior to application of the primary antibody the membrane was blocked with 2 % GE-block in PBS-T (PBS with 0.0075 % Tween-20) overnight at 4 °C under constant agitation. Incubation with mAb 1E8 for 1 h at ambient temperature was followed by 3 washing steps by 10 min incubation in PBS-T under constant

agitation. A biotinylated anti-mouse IgG antibody (Linaris) was applied for 45 min as secondary antibody. After another 3 washing steps with PBS-T, the blot was incubated with streptavidin-coupled horseradish peroxidase for 45 min at ambient temperature. Again 3 washing steps with PBS-T were performed, before the blots were developed using ECL-prime (GE-Healthcare) for 5 min at ambient temperature and signals were recorded with a LiCor® imager.

3 Results

3.1 Antibody specificity, comparative staining

Specificity of most primary antibodies used in this study has already been demonstrated by the respective supplier (table 1). In context of this study the specificity of the anti-Aβ38 pAb #218403 against the C-terminus was tested in immunohistochemistry using an immunoadsorption protocol. Preincubation of the anti-Aβ38 pAb with 1g of the Aβ peptide Aβ4-38 suppressed the staining almost completely, as seen in comparison with staining using the untreated antibody (not shown; see figure 1 of publication I).

Comparative stainings carried out using the polyclonal rabbit anti-Aβ38 antibody #218403 and the commercially available monoclonal rabbit anti-Aβ38 antibody BA1-13 revealed differences in immunoreactivity in both a case of SAD and in the 3xTg mouse model. Staining with the polyclonal anti-Aβ38 antibody #218403 resulted in vastly stronger immunoreactivity compared to staining with the mAb BA1-13. Spatial distribution of immunoreactivity however, was found to be similar (not shown; see suppl. figure 1 of publication I).

3.2 Sporadic Alzheimer's Disease

At first the deposition of the C-terminally truncated Aβ peptide Aβ38 was analyzed in a set of SAD and non-demented control cases using the anti-Aβ38 pAb #218403. General Aβ pathology was assessed by staining with the pan-Aβ mAb 4G8, which allowed for a comparison of Aβ38 depositions with the overall plaque pathology and degree of CAA present in the cases investigated (table 2). Vascular staining of Aβ38 could be detected, to a varying degree, in the majority (8/13) of SAD cases (figure 2 A,B). In addition, one of the analyzed non-demented control cases showed significant vascular depositions of Aβ38, too.

The study showed that a strong correlation between the severity of CAA and the amount of vascular Aβ38 exists in SAD. In contrast, immunoreactivity to extracellular Aβ38 was hardly observed and Aβ38 within NPs could only be faintly detected in two of the SAD cases (figure 2F), even though plaque pathology was significant in all SAD cases and some of the non-demented control cases.

To further investigate the deposition of C-terminally truncated Aβ species, additional immunohistochemistry studies on SAD and NDC cases were performed using monoclonal antibodies against Aβ37 (D2A6H), Aβ38 (326F1) and Aβ39 (D5Y9L). Again, general Aβ pathology was assessed by staining with the pan-Aβ antibody 4G8. In addition, staining with the mAb G210 allowed comparison of the C-terminally truncated Aβ peptides with Aβ40 (table 3). Staining with the anti-Aβ38 mAb 326F1 largely reproduced results of the

abovementioned experiments which were carried out using the polyclonal rabbit anti-Aβ38 antibody #218403.

Table 2: Data from publication I on depositions of Aβ38 in sporadic AD cases and non-demented control cases including demographic data and semiquantitative analysis. 4G8 antibody was used for evaluation of overall plaqueload and degree of cerebral amyloid angiopathy. The pAb #218403 was used for evaluation of Aβ38 depositions. Aβ staining intensity was rated as follows: - absent staining; (+) scarce staining, + weak staining, ++ moderate staining, +++ abundant staining.

				Aβ (4G8)		Aβ38 (#218403)	
Age	Sex	Braak	Diag.	NP	CAA	NP	CAA
88	F	IV	AD	++	+	-	-
84	F	IV	AD	++	-	-	-
86	M	IV	AD	+	++	-	-
79	F	IV	AD	++	+++	-	+
88	F	IV	AD	+	-	-	-
84	F	IV	AD	++	+	-	+
93	M	IV	AD	+	+++	-	++
92	M	IV	AD	++	+	-	+
92	F	IV	AD	++	++	-	+
91	F	IV	AD	++	++	-	+
91	M	IV	AD	+	+++	(+)	++
92	F	IV	AD	+	++	(+)	++
91	F	IV	AD	++	+	-	-
70	M	0	NDC	-	-	-	-
90	F	I	NDC	+	+	-	+
88	F	I	NDC	+	-	-	-
73	M	0	NDC	-	-	-	-
91	M	I	NDC	-	-	-	-
78	F	I	NDC	(+)	-	-	-
84	M	I	NDC	-	-	-	-
78	M	I	NDC	++	+	-	-
82	F	I	NDC	-	-	-	-

As shown above for Aβ38, depositions of the other two C-terminally truncated Aβ peptides Aβ37 and Aβ39 were detected in more than half of the SAD brains that were investigated. Interestingly none of the investigated NDC cases showed any immunoreactivity to Aβ37 or Aβ39. It became evident that all three C-terminally truncated Aβ species are primarily deposited within the vasculature in SAD and that the extent of depositions corresponded well to the overall level of CAA, the latter being assessed by 4G8 staining. Although in some cases meningeal vessels showed a more pronounced immunoreactivity than parenchymal vessels, depositions of C-terminally truncated Aβ peptides were found to be present in both leptomeningeal and parenchymal vessels in the majority of the affected SAD cases (figure 2A-D). Unlike Aβ40, the major Aβ species found in vascular amyloid, the shorter Aβ species Aβ37, Aβ38, and Aβ39 were hardly detected within NPs (figure 2E-G).

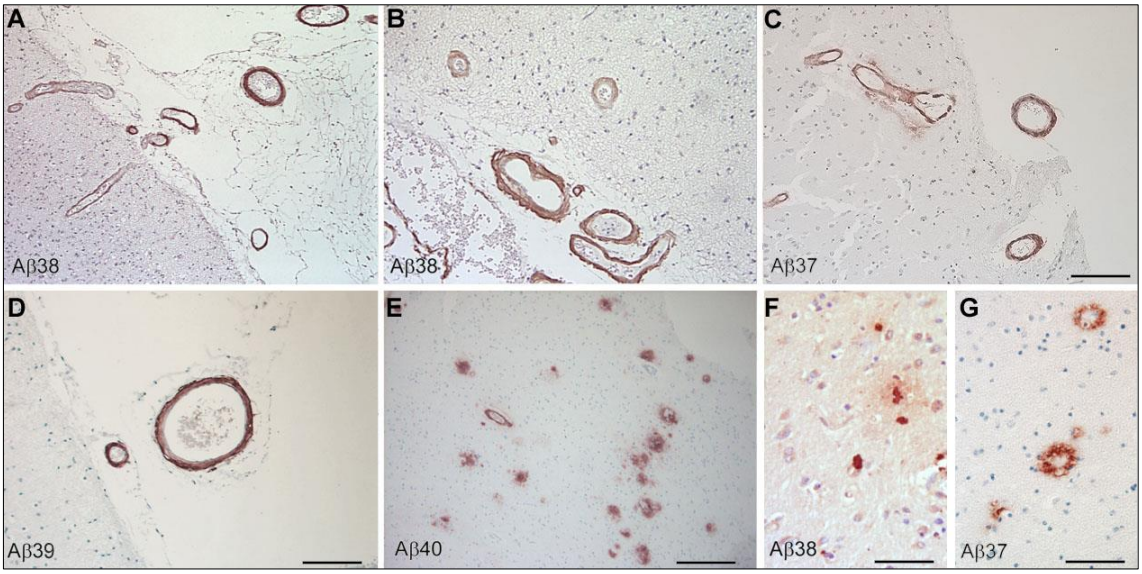

Figure 2: Immunohistochemical staining of SAD cases with antibodies against C-terminally truncated Aβ peptides and with anti-Aβ40 mAb G210. Staining of SAD cases using the anti-Aβ38 pAb revealed prominent immunoreactivity to Abeta38 in vascular compartments in the majority of the analyzed cases. Both parenchymal and leptomeningeal vessels were found to be affected (A,B). The same holds true for depositions of Aβ37 (C) and Aβ39 (D). Unlike the C-terminally truncated Aβ peptides, Aβ40 was found to be deposited within the vasculature and the parenchyma in most SAD cases (E). In contrast, parenchymal depositions of Aβ38 (F) and Aβ37 (G) were only detected infrequently and Aβ39 was not detected within NPs of SAD patients. Scale bars: A,C,D: 100 μm; B,E: 200 μm; F,G: 50 μm.

Double-immunofluorescence staining was carried out to evaluate co-localization of the vascular depositions of C-terminally truncated Aβ peptides with Aβ40. Aβ37 and Aβ38 were found to show either a partial or a complete co-localization with Aβ40 in the vessels of SAD patients. Aβ39 on the other hand, was found to show a different staining pattern from Aβ40 within most vessels (figure 3). Interestingly, prominent immunoreactivity to Aβ40 was seen in many vessels that did not show immunoreactivity to Aβ37, Aβ38, and Aβ39 respectively. This finding confirms that relevant cross-reactivity of the antibodies against the c-terminally truncated Aβ peptides with Aβ40 is unlikely (figure 3A-C). Due to the species of origin of the used antibodies, co-localization of the C-terminally truncated Aβ peptides could only be tested for Aβ38 and Aβ37 and for Aβ38 and Aβ39 but not for Aβ37 and Aβ39. Aβ38 was found to show either a partial or a complete overlap with Aβ37 and Aβ39 respectively (not shown; see figure 1 of publication II).

Table 3: Data from publication II with demographic data and semiquantitative analysis of staining intensity of the depositions of Aβ37, Aβ38, Aβ39, and Aβ40 in sporadic AD cases, Down Syndrome cases, and non-demented control cases. 4G8 antibody was used for the evaluation of overall plaqueload and degree of cerebral amyloid angiopathy. Names of the respective mAbs used for evaluation of depositions of Aβ37, Aβ38, Aβ39 and Aβ40 are set in brackets. Aβ staining intensity was rated as follows: - absent staining; (+) scarce staining, + weak staining, ++ moderate staining, +++ abundant staining.

				Aβ (4G8)		Aβ37 (D2A6H)		Aβ38 (326F1)		Aβ39 (D5Y9L)		Aβ40 (G210)	
Age	Sex	Braak	Diag.	NP	CAA	NP	CAA	NP	CAA	NP	CAA	NP	CAA
92	M	IV	AD	++	+	-	-	-	+	-	+	+	+
92	F	IV	AD	+	++	-	-	-	+	-	-	+	+
93	M	IV	AD	+	+++	-	+++	-	++	-	++	++	+++
91	M	IV	AD	++	+++	-	+	-	+	-	-	++	+++
84	F	IV	AD	++	+	-	+	-	++	-	++	+	++
91	F	IV	AD	++	++	-	++	(+)	+	-	+	++	+++
88	F	IV	AD	+	+	-	-	-	-	-	-	+	+
92	F	IV	AD	++	++	-	+	(+)	+	-	+	+	++
79	F	IV	AD	++	+++	(+)	++	(+)	+++	-	++	++	+++
84	F	IV	AD	++	-	-	-	-	-	-	-	+	-
91	F	IV	AD	++	+	-	(+)	-	-	-	(+)	(+)	+
86	M	IV	AD	+	++	-	+++	-	++	-	+++	+	++
88	F	IV	AD	++	+	-	-	-	-	-	-	-	+
96	F	V	AD+CAA	++	+++	-	+	-	+++	-	++	++	+++
82	F	V	AD+CAA	++	+++	-	++	-	+++	+	+++	+++	+++
61	F	VI	DS	++	-	-	-	-	-	-	-	+	-
58	M	VI	DS	++	++	(+)	+	+	+	-	-	++	++
64	F	V	DS	++	++	-	++	-	++	-	++	++	++
91	M	I	NDC	-	-	-	-	-	-	-	-	-	-
78	F	I	NDC	(+)	-	-	-	-	-	-	-	-	+
73	M	0	NDC	-	-	-	-	-	-	-	-	-	-
84	M	I	NDC	-	-	-	-	-	-	-	-	-	-
88	F	I	NDC	+	-	-	-	-	-	-	-	-	-
78	M	I	NDC	++	+	-	-	-	+	-	-	+	++
82	F	I	NDC	-	-	-	-	-	-	-	-	-	-
70	M	0	NDC	-	-	-	-	-	-	-	-	-	-

Two of the analyzed DS cases showed prominent CAA as assessed by 4G8 staining. While Aβ38 was detected in both meningeal and parenchymal vessels, Aβ37 and Aβ39 were found to be mainly present within meningeal vessels only. Aβ37, Aβ38, and Aβ39 were abundantly detected along with Aβ40 within vessels of the two analyzed cases with AD + CAA. Surprisingly one of the cases also showed faint immunoreactivity to Aβ39 in extracellular plaques (not shown; see suppl. figure 1 of publication II).

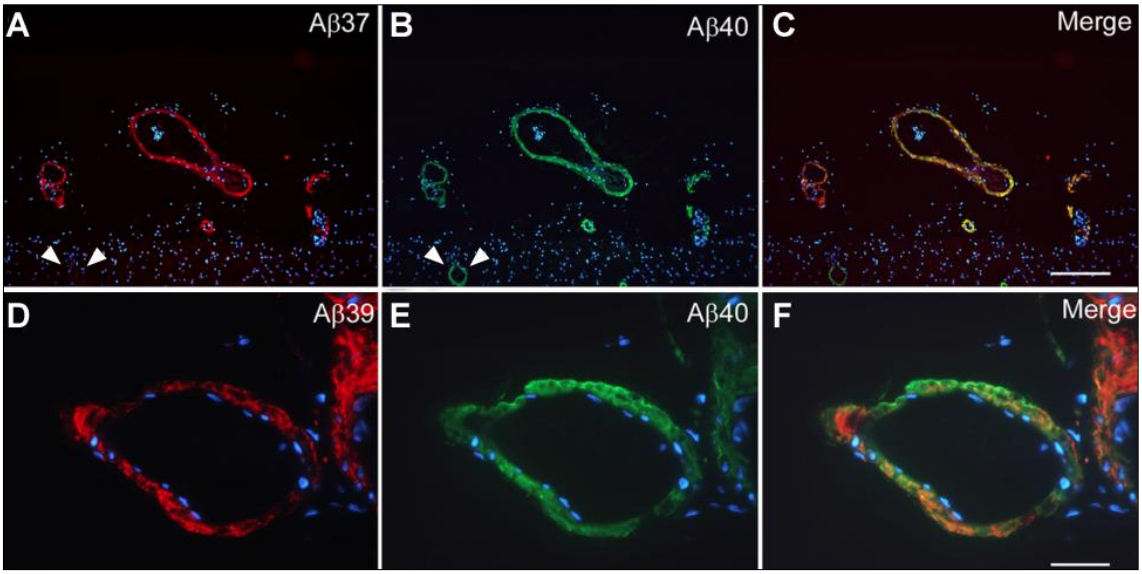

Figure 3: Double-Immunofluorescence was used to analyze co-localization of the C-terminally truncated Aβ peptides with Aβ40. Aβ37 (A-C) and Aβ38 (not shown, see figure 2D-I of publication I) were found to show either a partial or a complete overlap of staining patterns with Aβ40 in most affected vessels in SAD. White arrows indicate a vessel clearly detected by the anti-Aβ40 mAb G210 (B), while not showing fluorescence after staining by the anti-Aβ37 mAb D2A6H (A). Aβ39 was found to show a distinct staining pattern from Aβ40 in most vessels (D-F). Images have been published before in publication II (Reinert et al. Acta Neuropathologica Communications (2016) 4:24) under the terms of the Creative Commons Attribution 4.0 International License. As a modification to the original images white arrows have been added here. Scale bars: A-C: 200 μm; D-F: 100 μm

3.3 Familial Alzheimer's Disease

FAD cases with different underlying APP mutations and a case carrying the PSEN1 mutation ΔExon 9 were analyzed for depositions of C-terminally truncated Aβ peptides and Aβ40 and Aβ42 (table 4). Studies on Aβ38 in FAD included additional cases of FAD carrying mutations in PSEN1 (table 4).

Besides prominent depositions of the C-terminally truncated Aβ peptides in the vasculature, some of the FAD cases also exhibited significant immunoreactivity to the peptides in NPs. Especially Aβ37 could be detected within NPs, while Aβ38 was less abundant within NPs and Aβ39 was confined to the vasculature in most cases. Figure 4 shows a selection of images of the stainings that were performed in FAD cases, with special emphasis on Aβ38 (figure 4B, E-I). Further images are shown in figure 3 of publication I and figure 2 of publication II.

This study included analyses of a case of the recently described APP mutation I716F (Guardia-Laguarta et al. 2010). Presence of a wide range of Aβ peptides with varying C-termini was assessed using IHC for the first time. Similar to Aβ40, Aβ37 and Aβ38 (figure

4F) were predominantly present within the vasculature, while Aβ42 was found to be mainly deposited as NPs. In fact, staining of adjacent brain sections demonstrated that most of the NPs only exhibited immunoreactivity to Aβ42, but not to the C-terminally truncated Aβ peptides nor to Aβ40. In contrast, NPs of the hippocampal region also showed significant immunoreactivity to Aβ37, Aβ38, and Aβ40. Aβ39 depositions on the other hand, were barely detected in the studied APP I716F case and were confined to the vasculature.

Table 4: Data from publications I and II including demographic data and semiquantitative analysis of the deposition of C-terminally truncated Abeta peptides in cases of FAD. Comparison to overall plaquepathology and CAA as assessed by 4G8-staining or to Aβ42 depositions as assessed by pAb #218703. See table 2 of publication II for further information, including evaluation of Aβ40 depositions in FAD cases. *The anti-Aβ38 mAb 326F1 was used to analyze the case with the APP mutation I716F for Aβ38 depositions, while the other cases were analyzed for Aβ38 depositions using the anti-Aβ38 pAb #218403. Aβ staining intensity was rated as follows: - absent staining; (+) scarce staining, + weak staining, ++ moderate staining, +++ abundant staining.

				Aβ37 (D2A6H)		Aβ38* (#218403)		Aβ39 (D5Y9L)		Aβ / Aβ42 (4G8/#218703)	
Age	Sex	Gene	Mut.	NP	CAA	NP	CAA	NP	CAA	NP	CAA
										Aβ	
64	M	APP	E693G	++	++	+	++	+	++	+++	+++
61	F	APP	KM670/671NL	+	++	-	++	-	+	+++	+++
										Aβ42	
47	M	APP	I716F*	++	++	+	++	-	(+)	+++	+
61	M	PSEN1	ΔExon9	++	++	+	+	-	+	+++	(+)
69	M	PSEN1	ΔExon9	n/a	n/a	-	++	n/a	n/a	+++	(+)
64	M	PSEN1	ΔExon9	n/a	n/a	-	+	n/a	n/a	+++	(+)
										Aβ	
54	M	PSEN1	P264L	n/a	n/a	-	++	n/a	n/a	+++	+++
38	M	PSEN1	L418F	n/a	n/a	+	++	n/a	n/a	+++	+++

The APP mutation KM670/671NL ('Swedish'), which is caused by a mutation in close proximity to the β-secretase cleavage site and is known to increase overall Aβ production (Mullan et al. 1992), also exhibited severe CAA with abundant depositions of Aβ37, Aβ38, and Aβ39 within the vasculature. Comparison of Aβ37, Aβ38, and Aβ39 depositions in a case with the APP mutation KM670/671NL ('Swedish') showed similar spatial distribution of the peptides in most vessels (figure 4A-C).

Abundant depositions of C-terminally truncated Aβ peptides were found in a case of the APP mutation E693G ('Arctic'). The mutation that increases formation of Aβ oligomers most likely through a conformational change of the Aβ peptide (Nilsberth et al. 2001) led to significant depositions of Aβ37, Aβ38, and Aβ39 not only within the vessels but also

within NPs. Of all analyzed cases with FAD mutations it was the only case to exhibit Aβ39 immunoreactivity within NPs.

In a case of the PSEN1 mutation L418F significant immunoreactivity to Aβ38 was found in both the vasculature and amyloid plaques (figure 4H). In contrast analysis of a case of the PSEN1 mutation P264F only revealed vascular depositions of Aβ38 (figure 4G). This study further included the IHC analysis of three cases of PSEN-1 mutations for depositions of Aβ38. While Aβ38 was found in the vasculature in 3/3 analyzed cases of the PSEN-1 mutation ΔExon9, immunoreactivity to Aβ38 within amyloid plaques was only found in one of the three cases of the mutation (figure 4I). In adjacent sections Aβ38 showed an almost completely inverse staining pattern compared to Aβ42 in this case (not shown; see figure 3E, F of publication I). Further analysis of this case included staining for Aβ37, Aβ39, and Aβ40. While Aβ37, Aβ38, Aβ40, and Aβ42 could be detected to a varying degree within NPs in this case, Aβ39 immunoreactivity could only be detected at vascular lesions (not shown; see table 2 and figure 2G-I of publication II).

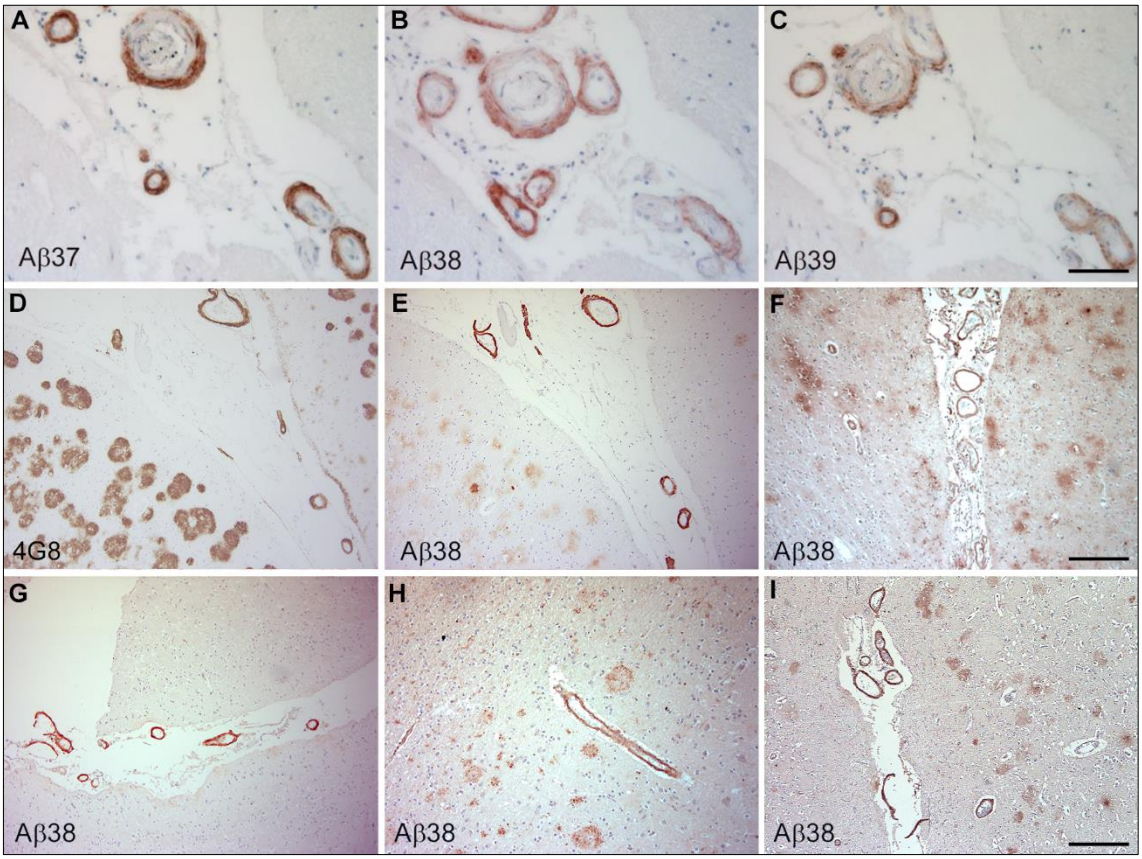

Figure 4: Selection of images showing IHC staining for C-terminally truncated Aβ peptides in FAD cases. Vascular depositions of C-terminally truncated Aβ37, Aβ38, and Aβ39 were observed in a case with the APP mutation KM670/671NL ('Swedish') (A-C). A case of the APP mutation E693G ('Arctic') showed abundant vascular and parenchymal depositions of Aβ as assessed by 4G8-staining (D), while Aβ38 depositions within NPs were less prominent (E). Further images show Aβ38 depositions within a case with the APP mutation I716F (F), a case with the PSEN1 mutation P264L (G), a case with the PSEN1 mutation L418F (H),

and a case with the PSEN 1 mutation ΔExon9 (I). Images A-C have been published before in published in publication II (Reinert et al. Acta Neuropathologica Communications (2016) 4:24) under the terms of the Creative Commons Attribution 4.0 International License. Scale bars: A-C: 200 μm; D-I: 100 μm

3.4 Transgenic Mouse Models

As part of this study a choice of 6 different mouse models of AD with different underlying mutations was investigated for depositions of the C-terminally truncated Aβ peptides. The results of IHC staining indicate that the C-terminally truncated peptides are generated and deposited in common mouse models of the disease (table 5).

Table 5: Data from publication II and publication I. Severity of extracellular Aβ depositions was assessed using the anti-Aβ37 mAb D2A6H, the anti-Aβ38 mAB 326F1, the anti-Aβ39 mAB D5Y9L, the anti-Aβ40 mAb G210. *The APP23 mouse model was analyzed for Aβ38 using the anti-Aβ38 pAb #218403. For more information on the analyzed mouse models see Table 2 of publication I. Aβ staining intensity was rated as follows: - absent staining; (+) scarce staining, + weak staining, ++ moderate staining, +++ abundant staining.

Transgenic model	Age	Aβ37	Aβ38*	Aβ39	Aβ40
APP/PSEN1ΔExon9	9 m	+	++	+	+++
5xFAD	7 m	+++	+++	+++	+++
PDAPP	18 m	+	+	+	++
APP23*	20 m	++	++	++	+++
3xTg	18 m	++	++	++	+++
APP/PSEN1-KI	10 m	+++	+++	+++	+++

In contrast to the staining pattern observed in SAD, immunoreactivity to C-terminally truncated Aβ peptides was found predominantly within NPs instead of within vessel walls. The investigated mouse models showed a correlation between the amount of immunoreactivity to the C-terminally truncated Aβ peptides and immunoreactivity to Aβ40. Depositions of C-terminally truncated Aβ peptides were most pronounced in the mouse models 5xFAD (figure 5) and APP/PSEN1-KI. Double-IF staining carried out in 7-month-old 5XFAD mice as well as 10-month-old APP/PSEN1-KI mice showed co-localization of Aβ37 and Aβ39 with Aβ40 in extracellular NPs (not shown; see suppl. figure 2 of publication II). Similarly, Aβ38 depositions in a 10-month-old APP/PSEN1-KI mouse were found to largely overlap with depositions of Aβ40 in the parenchyma, although a small vessel exhibited only partial co-localization of the two peptides (not shown; see figure 5K-N of publication I).

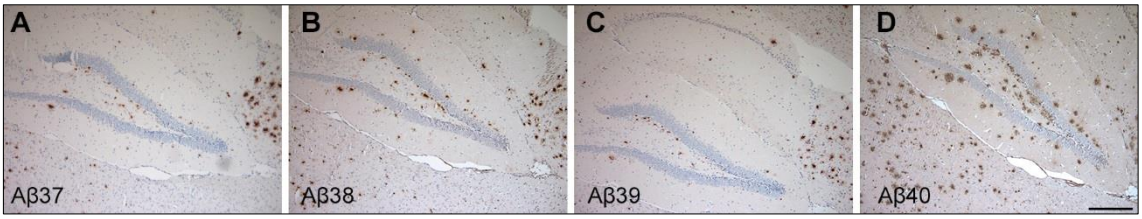

Figure 5: Images of IHC staining of depositions of Aβ37, Aβ38, Aβ39, and Aβ40 in adjacent sections at hippocampal region of the brain of a 7-month-old heterozygous 5xFAD mouse. Scale bar: 200 μm

C-terminally truncated Aβ peptides were also detected in lysates of brain tissue of 7-month-old heterozygous 5xFAD mice. A western blot was performed using anti-Aβ mAb 1E8, preceded by immunoprecipitation of Aβ peptides with anti-Aβ mAb 6E10 and a urea-based SDS-Page of the lysates. Alongside more distinct bands of Aβ 1-40 and Aβ 1-42, bands of Aβ 1-37, Aβ 1-38, and Aβ 1-39 were detected in both the TBS- and SDS-soluble fractions of the lysates (figure 6).

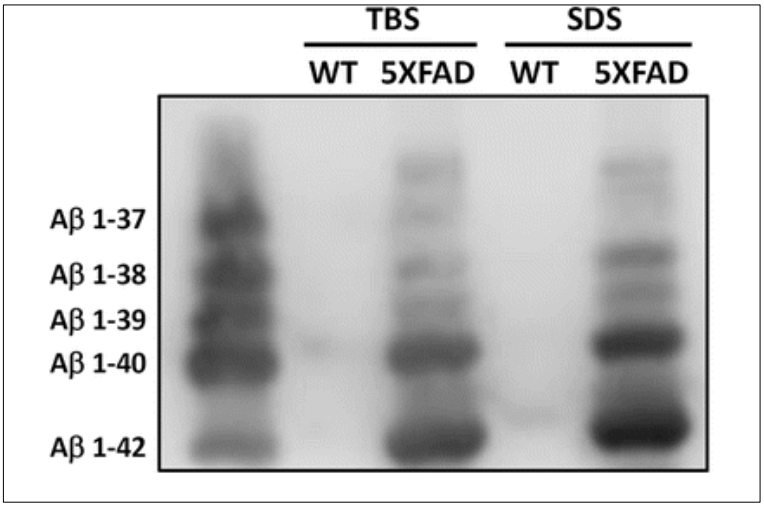

Figure 6: Western Blot for Aβ peptides in TBS- and SDS-soluble fractions from 7-month-old heterozygous 5xFAD and wild type (WT) mice. Prior to detection with 1E8 by Western Blot, Immunoprecipitation using 6E10 and a Urea-based SDS-Page were performed; comparison to a standard of Abeta peptides with varying C-terminus. Figure has been published before in publication II (Reinert J, Richard BC, Klafki HW, Friedrich B, Bayer TA, Wiltfang J, Kovacs GG, Ingelsson M, Lannfelt L, Paetau A et al. (2016): Deposition of C-terminally truncated Aβ species Aβ37 and Aβ39 in Alzheimer's disease and transgenic mouse models. Acta Neuropathologica Communications 4, 24) under the terms of the Creative Commons Attribution 4.0 International License.

4 Discussion

Despite the well-documented C-terminal heterogeneity of Aβ peptides, studies on the accumulation of Aβ peptides other than Aβ40 and Aβ42 are rare. The present study, for the first time, presents a comprehensive analysis of the depositions of a wide range of C-terminally truncated peptides in post-mortem tissue of patients affected by sporadic and familial AD. Comparison of Aβ37, Aβ38, and Aβ39 accumulations with overall Aβ pathology documents the severity and the predominant location of their depositions.

Although all of these peptides have been shown to occur in human CSF and blood plasma (Maler et al. 2007; Wiltfang et al. 2002; Welge et al. 2009) as well as within aqueous extracts of brain tissue (Portelius et al. 2010b), their involvement in the characteristic neuropathological changes in AD and in disease pathogenesis has not been thoroughly investigated. While absent from NDC cases, the three abovementioned C-terminally truncated peptides have been identified in a subset of AD cases and cases of pathologic aging in a recent Analysis using mass spectrometry of human brain lysates (Moore et al. 2012).

C-terminally truncated Aβ peptides have been shown to exhibit lower aggregation properties as compared to longer species (Vandersteen et al. 2012) and a high solubility in vitro (Schlenzig et al. 2012; Bouter et al. 2013). A study on FAD cases carrying the APP mutation D694N ('Iowa') found Aβ38 to represent a major fraction of Aβ species within the cerebrovascular compartment, while accounting for only a minor fraction of parenchymal Aβ (Tomidokoro et al. 2010). From this study, it can be inferred that Aβ38 is generally more likely to be found within vascular Aβ depositions rather than within NPs in AD patients.

Very recently Moro et al. reported results of immunohistochemical analyses of peptide depositions in the brains of AD patients that indeed found Aβ38 to be predominantly detectable within the vasculature. However, in SAD depositions of Aβ38 were found to be confined to a small subset of analyzed cases which exhibited severe CAA (Moro et al. 2012).

In good agreement with these findings, the study at hand shows Aβ38 to be mainly detectable within the vasculature of the SAD cases that were analyzed using the polyclonal rabbit anti-Aβ38 antibody #218403. In contrast to the aforementioned report by Moro et al., this study found Aβ38-immunoreactivity in the majority (8/13) of the analyzed SAD cases which harbored a varying degree of CAA. In addition, one of the nine analyzed NDC cases exhibited significant Aβ38-immunoreactivity within vessels of the brain. However, parenchymal depositions of the peptide were barely observed in SAD, as only two cases showed limited immunoreactivity to Aβ38 and only a low number of plaques were stained. Notably, the amount of vascular Aβ38 depositions in SAD was found to depend largely on the varying degree of CAA of the analyzed cases, as assessed by immunohistochemical staining with the anti-Aβ mAb 4G8. All the above was basically reproducible using the monoclonal mouse anti-Aβ38 antibody 326F1. This further confirms the results that were achieved using the polyclonal rabbit antibody. Minor differences in the results of the analyses

can be explained by (i) different section depth of the analyzed tissue or (ii) minor irregularities during staining protocol, e.g. insufficient exposure of the slice to the antibody due to unnoticed leakage of the applied solution from the slice during overnight incubation.

Comparative stainings were carried out with the anti-Aβ38 antibody used in the present (pAb #218403) and the one used in the previous study (mAb BA1-13) by Moro et al. It is conceivable that the observed differences in sensitivity of the antibodies account for the detection of Aβ38 in more cases of SAD in the present study as compared to the previous study.

As the present study was extended to include analyses of Aβ37 and Aβ39, it became evident that the vascular Aβ depositions in SAD contain a broad spectrum of C-terminally truncated Aβ peptides. Considering the fact that the severity of depositions of Aβ37 and Aβ39 in SAD was again found to correlate well with the degree of CAA in the analyzed cases, it can be concluded that the two peptides generally share a similar pattern of depositions with Aβ38. This was further confirmed by double-IF staining for Aβ37 and Aβ38 and for Aβ39 and Aβ38, which showed either partial or complete overlap of the vascular depositions in a case of SAD.

While Aβ37, Aβ38, and Aβ39 have essentially been confined to the vasculature in SAD, some of the analyzed FAD cases have been found to exhibit depositions of the peptides in the parenchyma as well. To allow insights into the mechanism involved in the generation of each C-terminally truncated Aβ peptide different APP mutations were chosen, located at the C-terminal part of Aβ (APP mutation I716F), at the N-terminal part of Aβ (APP mutation KM670/671NL 'Swedish') and within the Aβ-coding region (APP mutation E693G 'Arctic') (figure 1). This study further comprises analyses of PSEN1 mutations that have been shown to enhance accumulation by changing the spectrum of Aβ-peptides produced, thereby increasing the Aβ42:Aβ40 ratio. (Czech et al. 2000)

Based on observations made in FAD cases, it was hypothesized that Aβ38 depositions were specifically associated with those APP mutations that are found inside the Aβ-coding region of the APP gene, while APP mutations located adjacent to the Aβ-coding region did not favor accumulation of the peptide. In addition, several cases with underlying mutations in the presenilin genes were reported to lack Aβ38 depositions (Moro et al. 2012).

Although the present study confirms the occurrence of abundant vascular and parenchymal depositions of Aβ38 in a case with the APP mutation E693G ('Arctic'), it also found considerable accumulations of the peptide within the brains of patients with underlying APP mutations that are located outside of the Aβ coding region. These include a case of the APP mutation KM670/671NL ('Swedish'), which is located directly adjacent to the Aβ coding region of APP at the β-secretase cleavage site, and a case of the APP mutation I716F, which is located in proximity to the C-terminal sequence of Aβ. The case mentioned first exhibits prominent vascular depositions of the C-terminally truncated Aβ peptides including Aβ38,

the case with the underlying APP mutation I716F shows both vascular and parenchymal depositions of Aβ38.

Moreover, the present study shows Aβ38 to occur as both parenchymal and vascular depositions in patients with underlying mutations in the PSEN1 gene. While Aβ38 within NPs was only found in one patient carrying the PSEN1 mutation ΔExon9 and one patient carrying the PSEN1 mutation L418F, vascular Aβ38 depositions have been observed in all analyzed FAD cases with PSEN1 mutations. However, none of the PSEN1 mutations that have been analyzed here had previously been assessed for Aβ38 pathology and it is important to point out that it has been demonstrated that the generation of Aβ38 and Aβ42 can be differentially affected by different FAD causing PSEN mutation (Page et al. 2008). Therefore, the detection of Aβ38 depositions in the analyzed cases does not necessarily argue against the previous study which found no Aβ38 depositions in cases of FAD with other underlying PSEN1 mutations (Moro et al. 2012).

In conclusion though, the results of this study reject the assumption that Aβ38 might be limited to cases with underlying the intra-Aβ APP mutation in FAD and imply that Aβ38 depositions within the vasculature are commonly found in FAD and SAD.

Early studies on cerebrovascular Aβ already proposed that vascular Aβ, while homologous to plaque core Aβ, consists of shorter peptides made up of only 39 rather than 42 amino acids (Prelli et al. 1988). Later Aβ40 was shown to be the predominant species within cerebral vessels, while Aβ39 was found to account for a smaller fraction of vascular Aβ (Miller et al. 1993). Confirming these early results, the present study has found that depositions of Aβ39 are essentially limited to the vasculature. While Aβ37 and Aβ38 were also found in NPs of various analyzed FAD cases, parenchymal Aβ39 depositions were confined to one case carrying the intra-Aβ APP mutation E693G ('Arctic'). This mutation has been described to enhance aggregation propensities and hinder proteolytic degradation of Aβ (Nilsberth et al. 2001; Tsubuki et al. 2003). Intra-Aβ APP mutations in general have been described to present a distinct neuropathology that is characterized by severe CAA in most cases (Nilsberth et al. 2001). In line with this, the present study documents severe CAA in a case of the APP mutation E693G ('Arctic') and reveals great C-terminal heterogeneity of the deposited β-amyloids within both the vasculature and NPs.

While detection of numerous NPs by immunostaining for Aβ and by Bielschowsky silver staining has been reported for a case of the APP mutation I716F recently, characterization of Aβ deposition with respect to the C-terminus had not been carried out before (Sieczkowski et al. 2014). The present study has found abundant accumulations of Aβ peptides in a case of the APP mutation I716F, with Aβ42 representing the main species within NPs. This is in line with earlier studies that predicted the APP mutation I716F to cause extraordinary severe Aβ accumulation based on in vitro experiments (Lichtenthaler et al. 1999). There is profound evidence that the mutation causes immensely increased Aβ42 production mainly by a drastic change in Aβ42:Aβ40 ratio (Herl et al. 2009). This has been

interpreted to be a result of impaired γ-secretase cleavage, which purportedly leads to a shift in classic Aβ product lines. Hence the mutation has been proclaimed to favor the product line that includes production of Aβ42 (Aβ48 > Aβ45 > Aβ42 > Aβ38) over the product line leading primarily to production of Aβ40 (Aβ49 > Aβ46 > Aβ43 > Aβ40) (Suárez-Calvet et al. 2014). The present study shows significant Aβ38 depositions within vessels and parenchyma of the analyzed case, which can be explained with the common product line of Aβ42 and Aβ38. Yet the relatively scarce depositions of Aβ39 and the abundant depositions of Aβ37 – a species which has been found to primarily result from the release of GVV tripeptide from Aβ40 – might underscore recent findings about deviations from the major product lines of γ-secretase (Matsumura et al. 2014).

Surprisingly, Aβ37 was detected in NPs of all analyzed FAD cases with underlying APP mutation, and depositions were found to be more prominent than depositions of the other two analyzed C-terminally truncated Aβ peptides. This raises further questions about differences in properties of the three peptides and their ways of generation in FAD. Multiple pathways of successive γ-secretase cleavages have been described to lead to the formation of C-terminally truncated Aβ peptides. This includes the release of the GVVIA pentapeptide from Aβ42 that leads to the release of Aβ37 (Matsumura et al. 2014). It is possible that this γ-secretase action is responsible for the relative abundance of Aβ37 depositions in APP mutation carriers that exhibit high levels of Aβ42.

Although the C-terminally truncated Aβ peptides and Aβ40 exhibit similar aggregation propensities in vitro (Vandersteen et al. 2012), this study has found depositions of the C-terminally truncated Aβ peptides to be significantly less abundant in SAD than depositions of Aβ40. Undoubtedly part of this can be explained by the lower production rates of the C-terminally truncated peptides. It is interesting that depositions of the C-terminally truncated Aβ peptides within plaques were found to be almost confined to FAD cases. This could be explained by the generally more severe neuropathology that was documented for the analyzed cases in this study. Although this would need to be confirmed in additional studies it seems likely that the deposition of C-terminally truncated Aβ peptides to NPs represents a late event in the development of AD neuropathology.

While APP processing has been shown to primarily result in the formation of Aβ40, the C-terminally truncated Aβ peptides Aβ37, Aβ38, and Aβ39 have been found to be produced at lower rates comparable to that of Aβ42 (Younkin 1998; Suzuki et al. 1994; Beher et al. 2002). Subtle changes of production rates have been found to heavily influence the aggregation process of the resulting Aβ mixture. It has been proposed that the relative production rather than the absolute amount of toxic Aβ peptides is crucial for the aggregation of Aβ in vivo. In this regard the Aβ42:Aβ40 production ratio seems to be of particular importance (Kuperstein et al. 2010). Interestingly, Aβ40 has been found to hinder the aggregation of Aβ42 both in vitro and in mouse models of AD (Portelius et al. 2010b). On these grounds speculation about a putative protective role of Aβ40 has emerged (Kim et al. 2007; Jan et al.

2008), which has recently received further support by a study on the effect of different Aβ peptides on tau phosphorylation (Hu et al. 2014). A similar protective function of C-terminally truncated Aβ species has been put up for debate after findings of a massive decrease of Aβ37, Aβ38, and Aβ39 in the CSF of FAD cases (Portelius et al. 2010a).

In SAD the concentrations of the C-terminally truncated Aβ peptides within the CSF have been shown to increase in a disease-specific manner and a possible role as biomarkers for incipient AD has been proposed (Wiltfang et al. 2002). In this regard, subsequent research on CSF of SAD patients has rendered Aβ38 to be the most suitable among the C-terminally truncated Aβ peptides. Determination of the peptide's CSF concentration has been found to increase diagnostic specificity of CSF analysis if combined with measurements of tau, Aβ40, and Aβ42 (Welge et al. 2009). Certainly, the mechanisms behind the characteristic changes in CSF and the concomitant deposition of the Aβ peptides within the brain in SAD patients that have been observed in the present study are intertwined. This is underlined by the fact that depositions of C-terminally truncated Aβ peptides, while present in the majority of analyzed SAD cases, have hardly been detected in NDC cases.

This study has also found the C-terminally truncated Aβ species to be deposited within NPs in the brains of a set of widely used mouse models of AD. The presence of such peptides in transgenic lines had not been demonstrated before. Aβ 37, Aβ38, and Aβ39 have been found to be deposited to NPs in all analyzed mouse models; the severity of their depositions has been found to depend on the overall severity of plaque pathology exhibited by each analyzed mouse model. In contrast, vascular depositions have been found to be absent in most models, which is best explained by the fact that most models generally exhibit hardly any vascular Aβ depositions. Western Blot analysis of 5XFAD mice has revealed significantly less Aβ1-37, Aβ1-38, and Aβ1-39 compared to Aβ1-40 and Aβ1-42. However, their presence in mouse models might represent a potential read-out to assess efficacy of GSMs in vivo. For this purpose, a ratio of plaques with immunoreactivity to Aβ42 and plaques with immunoreactivity to Aβ37/38/39 after Immunohistochemical staining could be established. Alternatively, biochemical methods such as Mass spectrometry or ELISA could be employed to directly measure levels of the C-terminally truncated Aβ peptides.

5 Conclusion

Taken together, the study at hand provides evidence for the presence of a broad range of C-terminally modified Aβ peptides in SAD and FAD patients. In good agreement with earlier research on the solubility of the peptides, the predominant location of depositions of Aβ37, Aβ38, and Aβ39 has been found to be the vasculature. In SAD cases a clear correlation between severity of CAA and amount of accumulations of the peptides could be established. Parenchymal depositions have been found in some of the analyzed FAD cases. Interestingly, the underlying mutations have affected the accumulation of Aβ37, Aβ38, and Aβ39 differently. It is noteworthy that FAD mutations were generally found to cause significant vascular depositions of the C-terminally truncated Aβ peptides that were investigated in this study. As observed in the FAD cases, the Aβ depositions within NPs in brains of transgenic mouse models that are based on FAD causing mutations have been found to exhibit great C-terminal heterogeneity as well.

Additional studies are needed to further elucidate the exact role of C-terminally truncated Aβ peptides in AD pathogenesis including possible protective functions, effects of new AD treatments on their production, and the cause for the observed C-terminal heterogeneity in Aβ depositions.

6 Appendix

6.1 Copyright statement

6.2 Publications

Publication I:

Reinert J, Martens H, Huettenrauch M, Kolbow T, Lannfelt L, Ingelsson M, Paetau A, Verkkoniemi-Ahola A, Bayer TA, Wirths O (2014): Aβ38 in the brains of patients with sporadic and familial Alzheimer's disease and transgenic mouse models. J. Alzheimers Dis. 39, 871–881

This publication is available at IOS Press through http://dx.doi.org/10.3233/JAD-131373

Publication II:

Reinert J, Richard BC, Klafki HW, Friedrich B, Bayer TA, Wiltfang J, Kovacs GG, Ingelsson M, Lannfelt L, Paetau A et al. (2016): Deposition of C-terminally truncated Aβ species Aβ37 and Aβ39 in Alzheimer's disease and transgenic mouse models. Acta Neuropathologica Communications 4, 24

This publication is available at BMC through https://doi.org/10.1186/s40478-016-0294-7

7 References

Bansal S, Maurya IK, Yadav N, Thota CK, Kumar V, Tikoo K, Chauhan VS, Jain R (2016): C-Terminal Fragment Abeta32-37 Analogues Protect Against Abeta Aggregation-Induced Toxicity. ACS Chem Neurosci

Beher D, Wrigley, Jonathan D J, Owens AP, Shearman MS (2002): Generation of C-terminally truncated amyloid-beta peptides is dependent on gamma-secretase activity. J Neurochem 82, 563–575

Biffi A, Greenberg SM (2011): Cerebral Amyloid Angiopathy: A Systematic Review. J Clin Neurol 7, 1–9

Blennow K, de Leon, Mony J, Zetterberg H (2006): Alzheimer's disease. Lancet 368, 387–403

Blennow K, Mattsson N, Scholl M, Hansson O, Zetterberg H (2015): Amyloid biomarkers in Alzheimer's disease. Trends Pharmacol Sci 36, 297–309

Bouter Y, Dietrich K, Wittnam JL, Rezaei-Ghaleh N, Pillot T, Papot-Couturier S, Lefebvre T, Sprenger F, Wirths O, Zweckstetter M et al. (2013): N-truncated amyloid β (Aβ) 4-42 forms stable aggregates and induces acute and long-lasting behavioral deficits. Acta Neuropathol 126, 189–205

Braak H, Braak E (1991): Neuropathological stageing of Alzheimer-related changes. Acta Neuropathol 82, 239–259

Campion D, Flaman J-M, Brice A, Hannequin D, Dubois B, Martin C, Moreau V, Charbonnier F, Didierjean O, Tardieu S et al. (1995): Mutations of the presenilin I gene in families with early-onset Alzheimer's disease. Hum Mol Genet 4, 2373–2377

Casas C, Sergeant N, Itier JM, Blanchard V, Wirths O, van der Kolk N, Vingtdeux V, van de Steeg E, Ret G, Canton T et al. (2004): Massive CA1/2 neuronal loss with intraneuronal and N-terminal truncated Abeta42 accumulation in a novel Alzheimer transgenic model. Am J Pathol 165, 1289–1300

Corder EH, Am Saunders, Strittmatter WJ, Schmechel DE, Gaskell PC, Small GW, Roses AD, Haines JL, Pericak-Vance MA (1993): Gene dose of apolipoprotein E type 4 allele and the risk of Alzheimer's disease in late onset families. Science 261, 921–923

Czech C, Tremp G, Pradier L (2000): Presenilins and Alzheimer's disease: biological functions and pathogenic mechanisms. Prog Neurobiol 60, 363–384

Czirr E, Weggen S (2006): Gamma-secretase modulation with Abeta42-lowering nonsteroidal anti-inflammatory drugs and derived compounds. Neurodegener Dis 3, 298–304

Czirr E, Cottrell BA, Leuchtenberger S, Kukar T, Ladd TB, Esselmann H, Paul S, Schubenel R, Torpey JW, Pietrzik CU et al. (2008): Independent Generation of A 42 and A 38 Peptide Species by -Secretase. Journal of Biological Chemistry 283, 17049–17054

DGPPN/DGN-Leitlinie 2015 S3-Leitlinie "Demenzen" (Langversion - 1. Revision, August 2015). https://www.dgppn.de/publikationen/s3-leitlinie-demenzen.html; Accessed on 17.10.2016.

Ferri CP, Prince M, Brayne C, Brodaty H, Fratiglioni L, Ganguli M, Hall K, Hasegawa K, Hendrie H, Huang Y et al. (2005): Global prevalence of dementia: a Delphi consensus study. Lancet 366, 2112–2117

Funamoto S, Morishima-Kawashima M, Tanimura Y, Hirotani N, Saido TC, Ihara Y (2004): Truncated carboxyl-terminal fragments of beta-amyloid precursor protein are processed to amyloid beta-proteins 40 and 42. Biochemistry 43, 13532–13540

Gabelle A, Roche S, Gény C, Bennys K, Labauge P, Tholance Y, Quadrio I, Tiers L, Gor B, Chaulet C et al. (2010): Correlations between soluble α/β forms of amyloid precursor protein and Aβ38, 40, and 42 in human cerebrospinal fluid. Brain Res 1357, 175–183

Games D, Adams D, Alessandrini R, Barbour R, Berthelette P, Blackwell C, Carr T, Clemens J, Donaldson T, Gillespie F (1995): Alzheimer-type neuropathology in transgenic mice overexpressing V717F beta-amyloid precursor protein. Nature 373, 523–527

Garcia-Alloza M, Robbins EM, Zhang-Nunes SX, Purcell SM, Betensky RA, Raju S, Prada C, Greenberg SM, Bacskai BJ, Frosch MP (2006): Characterization of amyloid deposition in the APPswe/PS1dE9 mouse model of Alzheimer disease. Neurobiol Dis 24, 516–524

Glenner GG, Wong CW (1984): Alzheimer's disease: initial report of the purification and characterization of a novel cerebrovascular amyloid protein. Biochem Biophys Res Commun 120, 885–890

Golde TE, Eckman CB, Younkin SG (2000): Biochemical detection of Abeta isoforms: implications for pathogenesis, diagnosis, and treatment of Alzheimer's disease. Biochim Biophys Acta 1502, 172–187

Gorevic PD, Goni F, Pons-Estel B, Alvarez F, Peress NS, Frangione B (1986): Isolation and partial characterization of neurofibrillary tangles and amyloid plaque core in Alzheimer's disease: immunohistological studies. J Neuropathol Exp Neurol 45, 647–664

Gravina SA, Ho L, Eckman CB, Long KE, Otvos L, Younkin LH, Suzuki N, Younkin SG (1995): Amyloid β Protein (Aβ) in Alzheimeri's Disease Brain Biochemical and immunocytochemical analysis with antibodies specific for forms ending at Aβ40 or Aβ42(43). J Biol Chem 270, 7013–7016

Guardia-Laguarta C, Pera M, Clarimón J, Molinuevo JL, Sánchez-Valle R, Lladó A, Coma M, Gómez-Isla T, Blesa R, Ferrer I et al. (2010): Clinical, neuropathologic, and biochemical

profile of the amyloid precursor protein I716F mutation. J Neuropathol Exp Neurol 69, 53–59

Haass C, Selkoe DJ (2007): Soluble protein oligomers in neurodegeneration: lessons from the Alzheimer's amyloid beta-peptide. Nat Rev Mol Cell Biol 8, 101–112

Haass C, Kaether C, Thinakaran G, Sisodia S (2012): Trafficking and proteolytic processing of APP. Cold Spring Harb Perspect Med 2, a006270

Hardy J, Allsop D (1991): Amyloid deposition as the central event in the aetiology of Alzheimer's disease. Trends Pharmacol Sci 12, 383–388

Hardy J, Higgins G (1992): Alzheimer's disease: the amyloid cascade hypothesis. Science 256, 184–185

Hardy J, Selkoe DJ (2002): The amyloid hypothesis of Alzheimer's disease: progress and problems on the road to therapeutics. Science 297, 353–356

Haussmann U, Jahn O, Linning P, Janssen C, Liepold T, Portelius E, Zetterberg H, Bauer C, Schuchhardt J, Knolker HJ et al. (2013): Analysis of amino-terminal variants of amyloid-beta peptides by capillary isoelectric focusing immunoassay. Anal Chem 85, 8142–8149

Herl L, Thomas AV, Lill CM, Banks M, Deng A, Jones PB, Spoelgen R, Hyman BT, Berezovska O (2009): Mutations in amyloid precursor protein affect its interactions with presenilin/gamma-secretase. Mol Cell Neurosci 41, 166–174

Hu X, Li X, Zhao M, Gottesdiener A, Luo W, Paul S (2014): Tau pathogenesis is promoted by Aβ1-42 but not Aβ1-40. Mol Neurodegener 9, 1

Ida N, Hartmann T, Pantel J, Schroder J, Zerfass R, Forstl H, Sandbrink R, Masters CL, Beyreuther K (1996): Analysis of heterogeneous A4 peptides in human cerebrospinal fluid and blood by a newly developed sensitive Western blot assay. J Biol Chem 271, 22908–22914

Jan A, Gokce O, Luthi-Carter R, Lashuel HA (2008): The ratio of monomeric to aggregated forms of Abeta40 and Abeta42 is an important determinant of amyloid-beta aggregation, fibrillogenesis, and toxicity. J Biol Chem 283, 28176–28189

Jarrett JT, Berger EP, Lansbury, P T Jr (1993): The C-terminus of the beta protein is critical in amyloidogenesis. Ann N Y Acad Sci 695, 144–148

Kang J, Lemaire HG, Unterbeck A, Salbaum JM, Masters CL, Grzeschik KH, Multhaup G, Beyreuther K, Muller-Hill B (1987): The precursor of Alzheimer's disease amyloid A4 protein resembles a cell-surface receptor. Nature 325, 733–736

Kim J, Onstead L, Randle S, Price R, Smithson L, Zwizinski C, Dickson DW, Golde T, McGowan E (2007): Abeta40 inhibits amyloid deposition in vivo. J Neurosci 27, 627–633

Kuperstein I, Broersen K, Benilova I, Rozenski J, Jonckheere W, Debulpaep M, Vandersteen A, Segers-Nolten I, Van Der Werf, Kees, Subramaniam V et al. (2010): Neurotoxicity of

Alzheimer's disease Aβ peptides is induced by small changes in the Aβ42 to Aβ40 ratio. EMBO J 29, 3408–3420

Leitlinie Demenzen s. DGPPN/DGN-Leitlinie 2015

Lichtenthaler SF, Wang R, Grimm H, Uljon SN, Masters CL, Beyreuther K (1999): Mechanism of the cleavage specificity of Alzheimer's disease gamma-secretase identified by phenylalanine-scanning mutagenesis of the transmembrane domain of the amyloid precursor protein. Proc Natl Acad Sci USA 96, 3053–3058

Maler JM, Klafki H-W, Paul S, Spitzer P, Groemer TW, Henkel AW, Esselmann H, Lewczuk P, Kornhuber J, Wiltfang J (2007): Urea-based two-dimensional electrophoresis of beta-amyloid peptides in human plasma: evidence for novel Abeta species. Proteomics 7, 3815–3820

Markowitsch HJ, Staniloiu A (2012): Amnesic disorders. Lancet 380, 1429–1440

Masters CL, Simms G, Weinman NA, Multhaup G, McDonald BL, Beyreuther K (1985): Amyloid plaque core protein in Alzheimer disease and Down syndrome. Proc Natl Acad Sci. USA 82, 4245–4249

Matsumura N, Takami M, Okochi M, Wada-Kakuda S, Fujiwara H, Tagami S, Funamoto S, Ihara Y, Morishima-Kawashima M (2014): γ-Secretase associated with lipid rafts: multiple interactive pathways in the stepwise processing of β-carboxyl-terminal fragment. J Biol Chem 289, 5109–5121

McKhann GM, Knopman DS, Chertkow H, Hyman BT, Jack CR, JR, Kawas CH, Klunk WE, Koroshetz WJ, Manly JJ, Mayeux R et al. (2011): The diagnosis of dementia due to Alzheimer's disease: recommendations from the National Institute on Aging-Alzheimer's Association workgroups on diagnostic guidelines for Alzheimer's disease. Alzheimers Dement 7, 263–269

Miller DL, Papayannopoulos IA, Styles J, Bobin SA, Lin YY, Biemann K, Iqbal K (1993): Peptide compositions of the cerebrovascular and senile plaque core amyloid deposits of Alzheimer's disease. Arch Biochem Biophys 301, 41–52

Moro ML, Giaccone G, Lombardi R, Indaco A, Uggetti A, Morbin M, Saccucci S, Di Fede G, Catania M, Walsh DM et al. (2012): APP mutations in the Abeta coding region are associated with abundant cerebral deposition of Abeta38. Acta Neuropathol 124, 809–821

Mullan M, Crawford F, Axelman K, Houlden H, Lilius L, Winblad B, Lannfelt L (1992): A pathogenic mutation for probable Alzheimer's disease in the APP gene at the N-terminus of beta-amyloid. Nat Genet 1, 345–347

Myers RH, Schaefer EJ, Wilson PW, D'Agostino R, Ordovas JM, Espino A, Au R, White RF, Knoefel JE, Cobb JL et al. (1996): Apolipoprotein E epsilon4 association with dementia in a population-based study: The Framingham study. Neurology 46, 673–677

Nilsberth C, Westlind-Danielsson A, Eckman CB, Condron MM, Axelman K, Forsell C, Stenh C, Luthman J, Teplow DB, Younkin SG et al. (2001): The 'Arctic' APP mutation (E693G) causes Alzheimer's disease by enhanced Abeta protofibril formation. Nat Neurosci 4, 887–893

Norton S, Matthews FE, Barnes DE, Yaffe K, Brayne C (2014): Potential for primary prevention of Alzheimer's disease: an analysis of population-based data. Lancet Neurol 13, 788–794

Oakley H, Cole SL, Logan S, Maus E, Shao P, Craft J, Guillozet-Bongaarts A, Ohno M, Disterhoft J, van Eldik L et al. (2006): Intraneuronal beta-amyloid aggregates, neurodegeneration, and neuron loss in transgenic mice with five familial Alzheimer's disease mutations: potential factors in amyloid plaque formation. J Neurosci 26, 10129–10140

Oddo S, Caccamo A, Shepherd JD, Murphy MP, Golde TE, Kayed R, Metherate R, Mattson MP, Akbari Y, LaFerla FM (2003): Triple-transgenic model of Alzheimer's disease with plaques and tangles: intracellular Abeta and synaptic dysfunction. Neuron 39, 409–421

Olson MI, Shaw CM (1969): Presenile dementia and Alzheimer's disease in mongolism. Brain 92, 147–156

Page RM, Baumann K, Tomioka M, Perez-Revuelta BI, Fukumori A, Jacobsen H, Flohr A, Luebbers T, Ozmen L, Steiner H et al. (2008): Generation of Abeta38 and Abeta42 is independently and differentially affected by familial Alzheimer disease-associated presenilin mutations and gamma-secretase modulation. J Biol Chem 283, 677–683

Perez-tur J, Froelich S, Prihar G, Crook R, Baker M, Duff K, Wragg M, Busfield F, Lendon C, Clark RF (1995): A mutation in Alzheimer's disease destroying a splice acceptor site in the presenilin-1 gene. Neuroreport 7, 297–301

Portelius E, Andreasson U, Ringman JM, Buerger K, Daborg J, Buchhave P, Hansson O, Harmsen A, Gustavsson MK, Hanse E et al. (2010a): Distinct cerebrospinal fluid amyloid beta peptide signatures in sporadic and PSEN1 A431E-associated familial Alzheimer's disease. Mol Neurodegener 5, 2

Portelius E, Bogdanovic N, Gustavsson MK, Volkmann I, Brinkmalm G, Zetterberg H, Winblad B, Blennow K (2010b): Mass spectrometric characterization of brain amyloid beta isoform signatures in familial and sporadic Alzheimer's disease. Acta Neuropathol 120, 185–193

Prelli F, Castano E, Glenner GG, Frangione B (1988): Differences between vascular and plaque core amyloid in Alzheimer's disease. J Neurochem 51, 648–651

Prince M: World Alzheimer report 2015: The global impact of dementia an analysis of prevalence, incidence, cost and trends, [Revised edition]; Alzheimer's Disease International, London 2015

Qi-Takahara Y, Morishima-Kawashima M, Tanimura Y, Dolios G, Hirotani N, Horikoshi Y, Kametani F, Maeda M, Saido TC, Wang R et al. (2005): Longer forms of amyloid beta protein: implications for the mechanism of intramembrane cleavage by gamma-secretase. J. Neurosci 25, 436–445

Saul A, Lashley T, Revesz T, Holton J, Ghiso JA, Coomaraswamy J, Wirths O (2013): Abundant pyroglutamate-modified ABri and ADan peptides in extracellular and vascular amyloid deposits in familial British and Danish dementias. Neurobiol. Aging 34, 1416–1425

Savastano A, Klafki H, Haussmann U, Oberstein TJ, Muller P, Wirths O, Wiltfang J, Bayer TA (2015): N-Truncated Abeta 2-X Starting with Position Two in Sporadic Alzheimer's Disease Cases and Two Alzheimer Mouse Models. J Alzheimers Dis 49,101-110

Schlenzig D, Rönicke R, Cynis H, Ludwig H-H, Scheel E, Reymann K, Saido T, Hause G, Schilling S, Demuth H-U (2012): N-Terminal pyroglutamate formation of Aβ38 and Aβ40 enforces oligomer formation and potency to disrupt hippocampal long-term potentiation. J. Neurochem 121, 774–784

Schoonenboom NS, Mulder C, van Kamp GJ, Mehta SP, Scheltens P, Blankenstein MA, Mehta PD (2005): Amyloid β 38, 40, and 42 species in cerebrospinal fluid: More of the same? Ann Neurol 58, 139–142

Selkoe DJ (2001): Alzheimer's disease: genes, proteins, and therapy. Physiol Rev 81, 741–766

Selkoe DJ, Hardy J (2016): The amyloid hypothesis of Alzheimer's disease at 25 years. EMBO Mol Med 8, 103-114

Sieczkowski E, Milenkovic I, Venkataramani V, Giera R, Ströbel T, Höftberger R, Liberski PP, Auff E, Wirths O, Bayer TA et al. (2014): I716F AβPP Mutation Associates with the Deposition of Oligomeric Pyroglutamate Amyloid-β and α-Synucleinopathy with Lewy Bodies. J Alzheimers Dis 44, 103-114

Slooter AJ, Cruts M, Hofman A, Koudstaal PJ, van der Kuip D, Ridder MA de, Witteman JC, Breteler MM, van Broeckhoven C, van Duijn CM (2004): The impact of APOE on myocardial infarction, stroke, and dementia: the Rotterdam Study. Neurology 62, 1196–1198

Strooper Bd, Saftig P, Craessaerts K, Vanderstichele H, Guhde G, Annaert W, Figura K von, van Leuven F (1998): Deficiency of presenilin-1 inhibits the normal cleavage of amyloid precursor protein. Nature 391, 387–390

Struyfs H, van Broeck B, Timmers M, Fransen E, Sleegers K, van Broeckhoven C, Deyn PP de, Streffer, JR, Mercken M, Engelborghs S (2015): Diagnostic Accuracy of Cerebrospinal Fluid Amyloid-beta Isoforms for Early and Differential Dementia Diagnosis. J Alzheimers Dis 45, 813–822

Sturchler-Pierrat C, Abramowski D, Duke M, Wiederhold KH, Mistl C, Rothacher S, Ledermann B, Bürki K, Frey P, Paganetti PA et al. (1997): Two amyloid precursor protein

transgenic mouse models with Alzheimer disease-like pathology. Proc Natl Acad Sci USA 94, 13287–13292

Suárez-Calvet M, Belbin O, Pera M, Badiola N, Magrané J, Guardia-Laguarta C, Muñoz L, Colom-Cadena M, Clarimón J, Lleó A (2014): Autosomal-dominant Alzheimer's disease mutations at the same codon of amyloid precursor protein differentially alter Aβ production. J Neurochem 128, 330–339

Suzuki N, Cheung T, Cai X, Odaka A, Otvos L, Eckman C, Golde T, Younkin S (1994): An increased percentage of long amyloid beta protein secreted by familial amyloid beta protein precursor (beta APP717) mutants. Science 264, 1336–1340

Takami M, Nagashima Y, Sano Y, Ishihara S, Morishima-Kawashima M, Funamoto S, Ihara Y (2009): gamma-Secretase: successive tripeptide and tetrapeptide release from the transmembrane domain of beta-carboxyl terminal fragment. J Neurosci 29, 13042–13052

Tanzi RE (2012): The genetics of Alzheimer disease. Cold Spring Harb Perspect Med 2

Tanzi RE, Gusella JF, Watkins PC, Bruns GA, St G-HP, van Keuren ML, Patterson D, Pagan S, Kurnit DM, Neve RL (1987): Amyloid beta protein gene: cDNA, mRNA distribution, and genetic linkage near the Alzheimer locus. Science 235, 880–884

Tomidokoro Y, Rostagno A, Neubert TA, Lu Y, Rebeck GW, Frangione B, Greenberg SM, Ghiso J (2010): Iowa Variant of Familial Alzheimer's Disease. Am J Pathol 176, 1841–1854

Tsubuki S, Takaki Y, Saido TC (2003): Dutch, Flemish, Italian, and Arctic mutations of APP and resistance of Abeta to physiologically relevant proteolytic degradation. Lancet 361, 1957–1958

van Duijn CM, Clayton D, Chandra V, Fratiglioni L, Graves AB, Heyman A, Jorm AF, Kokmen E, Kondo K, Mortimer JA et al. (1991): Familial aggregation of Alzheimer's disease and related disorders: a collaborative re-analysis of case-control studies. Int J Epidemiol 20 Suppl 2, S13-20

Vandersteen A, Hubin E, Sarroukh R, Baets G de, Schymkowitz J, Rousseau F, Subramaniam V, Raussens V, Wenschuh H, Wildemann D et al. (2012): A comparative analysis of the aggregation behavior of amyloid-β peptide variants. FEBS Lett 586, 4088–4093

Villemagne VL, Burnham S, Bourgeat P, Brown B, Ellis KA, Salvado O, Szoeke C, Macaulay SL, Martins R, Maruff P et al. (2013): Amyloid beta deposition, neurodegeneration, and cognitive decline in sporadic Alzheimer's disease: a prospective cohort study. Lancet Neurol 12, 357–367

Weggen S, Eriksen JL, Das P, Sagi SA, Wang R, Pietrzik CU, Findlay KA, Smith TE, Murphy MP, Bulter T et al. (2001): A subset of NSAIDs lower amyloidogenic Aβ42 independently of cyclooxygenase activity. Nature 414, 212–216

Welge V, Fiege O, Lewczuk P, Mollenhauer B, Esselmann H, Klafki H-W, Wolf S, Trenkwalder C, Otto M, Kornhuber J et al. (2009): Combined CSF tau, p-tau181 and amyloid-β 38/40/42 for diagnosing Alzheimer's disease. J Neural Transm 116, 203–212

Wiltfang J, Smirnov A, Schnierstein B, Kelemen G, Matthies U, Klafki HW, Staufenbiel M, Huther G, Ruther E, Kornhuber J (1997): Improved electrophoretic separation and immunoblotting of beta-amyloid (A beta) peptides 1-40, 1-42, and 1-43. Electrophoresis 18, 527–532

Wiltfang J, Esselmann H, Bibl M, Smirnov A, Otto M, Paul S, Schmidt B, Klafki H-W, Maler M, Dyrks T et al. (2002): Highly conserved and disease-specific patterns of carboxyterminally truncated Abeta peptides 1-37/38/39 in addition to 1-40/42 in Alzheimer's disease and in patients with chronic neuroinflammation. J Neurochem 81, 481–496

Wirths O, Erck C, Martens H, Harmeier A, Geumann C, Jawhar S, Kumar S, Multhaup G, Walter J, Ingelsson M et al. (2010): Identification of low molecular weight pyroglutamate Abeta oligomers in Alzheimer disease: a novel tool for therapy and diagnosis. J Biol Chem 285, 41517–41524

Younkin SG (1998): The role of Aβ42 in Alzheimer's disease. Xth International Symposium on Cholinergic Mechanisms, Part III 92, 289–292